NASA TECHNICAL TRANSLATION NASA TTF-12,356

NASA TT F-12,356

TURBULENT BOUNDARY LAYER IN THE INITIAL SECTION OF A TUBE UNDER CONDITIONS OF NONISOTHERMICITY AND BLOWING

A.I. Leont'yev, A.V. Fafurin, P.V. Nikitin

Translation of: "Turbulentnyy pogranichnyy sloy v nachal'nom uchastke truby v usloviyakh neizotermichnosti i vduva"
Teplofizika vysokikh temperatur,
Vol. 7, No. 2, 1969, pp. 276-283

NATIONAL AERONAUTICS AND SPACE ADMINISTRATION
WASHINGTON, D.C. AUGUST, 1969

NASA TTF-12,356

TURBULENT BOUNDARY LAYER IN THE INITIAL SECTION OF A TUBE UNDER CONDITIONS OF NONISOTHERMICITY AND BLOWING

A.I. Leont'yev, A.V. Fafurin, P.V. Nikitin

ABSTRACT: This article presents theoretical and experimental investigations of a turbulent boundary layer in the initial section of a tube in the presence of nonisothermicity and blowing. The results of experiments, obtained in the range of Reynolds numbers from $6.14 \cdot 10^4$ to $9.61 \cdot 10^4$ and flow densities from 0 to 0.296, show a satisfactory correlation of the proposed method with the experimental method.

There has recently been increased interest in the investigation /27 of the influence of nonisothermicity and blowing on friction and heat exchange in a turbulent boundary layer. This interest has been primarily caused by research into means of heat shielding of surfaces streamlined by a flow of hot gases. In the literature there are references devoted to the study of this problem as applied to conduits of circular cross section. However, these references discuss the influence of blowing on a turbulent boundary layer which has already developed.

In this article we will make theoretical and experimental investigations of the influence of nonisothermicity and a lateral flow of matter on friction, heat exchange and also the gas parameters in the nucleus of the flow in the initial section of a cylindrical tube. We will derive formulas for calculating the coefficients of friction and heat exchange along the length of the stabilization section in the area of subsonic flow with a uniform distribution of gas parameters at the entrance to the tube.

In this case the system of initial equations has the form [3]:

The impulse equation:

$$\frac{dR^{**}}{dX}+(1+H)\frac{R^{**}}{W_0}\frac{dW_0}{dX}=W_0\frac{c_{f_0}}{2}(\Psi+b). \tag{1}$$

The continuity equation:

$$4HR^{**}=W_0-1-4\int_0^x j_1\,dX; \tag{2}$$

$$R^{**} = \rho_0 w_0 \delta^{++}/\mu_w R_1, \quad R_1 = \rho_{01} w_{01} D/\mu_w, \quad W_0 = w_0/w_{01},$$
$$\frac{c_{f_0}}{2} = \tau_{w_0}/\rho_0 w_0^2, \quad H = \delta^*/\delta^{**}, \quad b = j2/c_{f_0},$$
$$j = (\rho w)_w / \rho_0 w_0, \quad X = x/D, \quad \Psi = (c_f / c_{f_0})_{R^{**}}. \tag{3}$$

We will determine the relative coefficient of friction Ψ from the asymptotic formula, obtained in reference [4]:

$$\Psi = \left(\frac{2}{\sqrt{\psi_h}+1}\right)^2 \left(1 - \frac{b}{b_{cr}}\right)^2,$$
$$\left(b_{cr} = \frac{1}{1-\psi_h}\left(\ln\frac{1+\sqrt{1-\psi_h}}{1-\sqrt{1-\psi_h}}\right)^2 \quad \text{for} \quad \psi_h < 1;\right. \tag{4}$$
$$b_{cr} = \frac{1}{\psi_h - 1}\left(\arccos\frac{2-\psi_h}{\psi_h}\right)^2 \quad \text{for} \quad \psi_h > 1,$$

where $\psi_h = h_w/h_0$. /27

To solve system (1)-(4) we must know the relationship between the shape factor H and the nonisothermicity and the permeability factor. This relationship can be found if we take advantage of the integral equation for the dimensionless velocity, which was obtained in reference [4]:

$$\int_{\omega}^{1} \frac{d\omega}{\sqrt{(\Psi + b\omega)\rho_0/\rho}} = Z, \quad \omega = \frac{w}{w_0}. \tag{5}$$

Taking the similarity of the enthalpy and velocity profiles, we have

$$\rho_0/\rho = \psi_h + (1-\psi_h)\omega. \tag{6}$$

Substituting (6) into (5) and integrating for $\psi_h < 1$, we obtain the velocity profile in the turbulent nucleus of the boundary layer as a function of the permeability parameter

$$\omega = (k^2 - ac)/a(2k + d). \tag{7}$$

Here

$$a = (1-\psi_h)b, \quad d = (1-\psi_h)\Psi + \psi_h b, \quad c = \psi_h \Psi,$$
$$k = [\sqrt{a(a+d+c)} + a + {}^1/_2 d]\exp[-Z\sqrt{a}] - {}^1/_2 d. \tag{8}$$

Following reference [4], we posit that $Z = 1 - \omega_0$ where ω_0 is the velocity profile in a turbulent boundary layer under isothermic conditions in the absence of blowing, i.e., $\omega_0 = \xi^n$.

We can then obtain the velocity distribution across the boundary layer with a given permeability parameter, and, according to the known velocity profile and density profile, we can compute the integral characteristics δ^*, δ^{**} and H, i.e.

$$\delta^* = \int_0^\delta \left(1 - \frac{\rho}{\rho_0}\omega\right)\left(1 - \frac{y}{r_0}\right) dy,$$

$$\delta^{**} = \int_0^\delta \frac{\rho}{\rho_0}\omega(1-\omega)\left(1 - \frac{y}{r_0}\right) dy, \tag{9}$$

$$H = \frac{\delta^*}{\delta^{**}}.$$

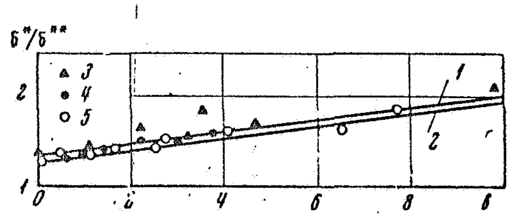

Fig. 1: The influence of the Permeability Factor b on the Shape Factor H:
1. For a Tube; 2. For a Plate; 3. [5]; 4. [6]; 5. The Data of the Authors; the Straight Line Shows the Calculation By Equation (10) for $k = 0.05$.

Figure 1 shows the results of the calculation of the shape factor H by the proposed method. The figure also shows the experimental data of references [5,6], obtained with nongradient streamlining of a flat plate by an isothermic flow and the data of the authors obtained with an isothermic flow in a circular tube with permeable walls (a description of the experiment is given below). It can be seen that the results of the calculations show a satisfactory correlation to the experimental data and can be approximated by the single function

$$H = H_0 \psi_h (1 + kb), \tag{10}$$

where H_0 is the value of the shape factor under isothermic conditions and $dp/dX = 0$, k is a constant.

Under standard conditions the coefficient of friction can be expressed by the function [4]

$$c_{f_0} = BR^{**-m} R_1^{-m}. \tag{11}$$

Then we obtain the following system of equations for a gas flow in the initial section of the tube: /278

$$\frac{dR^{**}}{dX}+(1+H)\frac{R^{**}}{W_0}\frac{dW_0}{dX}=W_0\frac{B}{2}(R^{**}R_1)^{-m}(\Psi+b),$$
$$4HR^{**}=W_0-1-4\int_0^x jR_1^m W_0 d\left(\frac{X}{R_1^m}\right),\tag{12}$$
$$b=jR_1^m\frac{2}{B}R^{**m}.$$

We will now examine two particular solutions to this system (a) b = const., ψ_h = const.

In this case we are able to obtain an analytic relationship between the Reynolds number, the velocity W_0

$$R^{**}=\frac{\Psi+b}{4\{b(2+H)+H(\Psi+b)\}}\cdot\frac{W_0^{\alpha+1}-1}{W_0^{\alpha}},$$
$$\alpha=\frac{(1+H)b}{b+H(\Psi+b)}\tag{13}$$

and the longitudinal coordinate

$$\frac{X}{R_1^m}=\frac{2(\Psi+b)^m}{B\{4[b(2+H)+H(\Psi+b)]\}^{1+m}}\int_1^{W_0}\left\{(2+H)\frac{(W_0^{\alpha+1}-1)^m}{W_0^{\alpha m+1}}-\right.$$
$$\left.-(1+H-\alpha)\frac{(W_0^{\alpha+1}-1)^m}{W_0^{\alpha(m+1)+2}}\right\}dW_0;\tag{14}$$

when b = 0 and m = 0.25, we obtain from (14) the known result [4]

$$\left[(1+H)\frac{5}{4}+1\right]\left[4(W_0-1)^{0,25}-\right.$$
$$-\frac{1}{\sqrt{2}}\ln\frac{(W_0-1)^{0,5}+\sqrt{2}(W_0-1)^{0,25}+1}{(W_0-1)^{0,5}-\sqrt{2}(W_0-1)^{0,25}+1}-\tag{15}$$
$$\left.-\sqrt{2}\arctan\frac{\sqrt{2}(W_0-1)^{0,25}}{1-(W_0-1)^{0,5}}\right]-(1+H)\frac{(W_0-1)^{1,25}}{W_0}=$$
$$=\Psi\frac{0,0725H^{1,25}}{R_1^{0,25}}X.$$

We should note here that the obtained relationships are valid only for the initial section of the tube, while the boundary layer has not yet collapsed. We will determine the length of the initial section from the condition that at the end of the stabilization section the thickness of the boundary layer is equal to the radius of the tube. Then

$$R_{1}^{**} = R^{1}/_{2}\delta^{**} / r_0 = R_1{}^{1}/_{2}W_{01}\delta^{**} / r_0. \tag{16}$$

Simultaneously solving (13) and (16), we obtain

$$W_{01} = \left(\frac{1}{1-S}\right)^{\beta},$$
$$S = \left(2\frac{r_0}{\delta^{**}}\frac{\Psi + b}{4\{b(2+H)+H(\Psi+b)\}}\right)^{-1}, \quad \beta = \frac{1}{1+\alpha}. \tag{17}$$

Figure 2 shows the results of the calculation of the relative velocity distribution under isothermic conditions along the length of the initial section as a function of the permeability factor for various values of *b*. It is clear that blowing has a considerable effect on the value of the velocity in the nucleus of the flow. Here the broken line refers to the boundary of the initial section, as computed by (14) and (17). /27

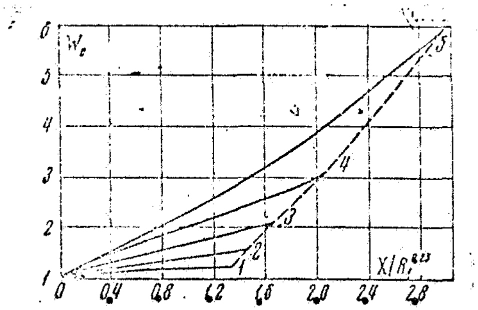

Fig. 2: The Relative Velocity Distribution W_0 Along the Length of the Initial Section of the Tube for *b*: (1) 0;(2) 1;(3) 2:(4) 3:(5) 4 (The Broken Line Refers to the Boundary of the Initial Section)

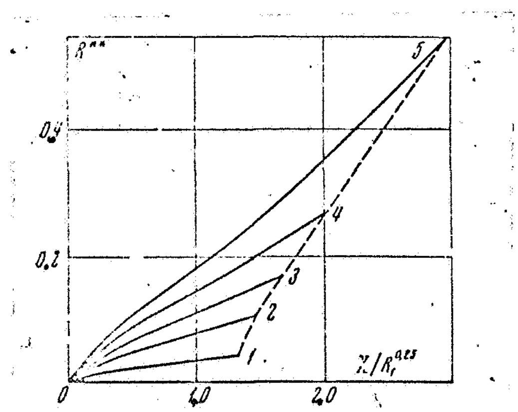

Fig. 3: The Change in the Reynolds Number Along the Length of the Tube (for the Notations, See Fig. 2)

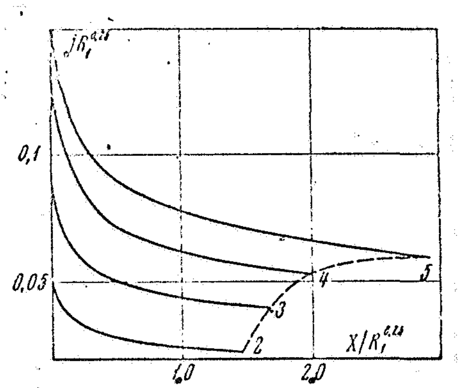

Fig. 4: The Relative Blowing Distribution Along the Length of the Tube (for the Notations, see Fig. 2).

Figures 3 and 4 show the change in the Reynolds number and in the relative blowing for the same values of the permeability factor.

(b) $j_1 = (\rho w)_w/(\rho_{01} w_{01}) = \text{const.}$

In this case system (12) can be reduced to the relationships

$$\frac{dR^{**}}{dW_0} = \frac{1 + 4kbH_0R^{**}/W_0 - (1+H)4b(\Psi+b)^{-1}R^{**}/W_0}{4kmbH_0 + 4H + 4b(\Psi+b)^{-1}}; \tag{18}$$

$$X/R_1^m = (W_0 - 1 - 4HR^{**})/4j_1R_1^m; \tag{19}$$

$$b = j_1R_1^mR^{**m}/W_0, \tag{20}$$

where the relationship between the number R^{**} and the relative velocity W_0 can be found from the numerical solution of equation (18)

Figures 5 and 6 show the results of the calculation of the relative velocity and the Reynolds number as a function of the longitudinal coordinate for various values of the flow density $j_1R_1^{0.25}$. Equation (18) was solved numerically on a computer by the Runge-Kutta method and then checked with $j_1R_1^{0.25} = 0$ by a change in the integration step. The broken line in these figures, showing the boundary of the initial section, was computed by simultaneous solution of equations (16), (18).

Figure 7 shows the change in the permeability factor b along the length of the initial section under the given conditions.

For an experimental investigation of this problem, we constructed an experimental apparatus, a diagram of which is shown in Figure 8. /280

The experimental section was constructed of a porous titanium tube with an internal diameter of 34.5 mm. The thickness of the walls was 2 mm and the length was 346 mm.

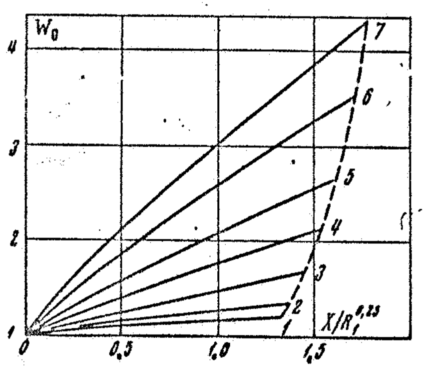

Fig. 5: Distribution of the Relative Velocity Along the Length of the Initial Section of the Tube for $j_1 R_1^{0.25}$: (1) 0; (2) 0.02; (3) 0.05; (4) 0.10; (5) 0.15; (6) 0.23; (7) 0.296 (The Broken Line Refers to the Boundary of the Initial Section).

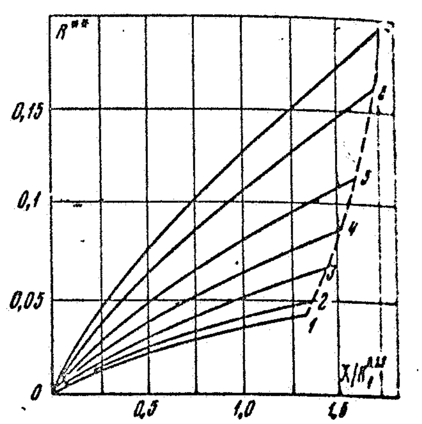

Fig. 6: The Reynolds Number as a Function of the Length of the Tube and the Density of the Lateral Flow of Matter (For the Notation, See Fig. 5).

The diameter of the powder particles was about 0.063 mm. Before the main experiments, we investigated the hydraulic characteristics for determination of the flow rate of the refrigerant as a function of the pressure drop on a sample. In addition, we verified the uniformity of the permeability along the length of the tube in its four diametrically placed generating lines using a thermal anemometer. The diameter of the filament of the thermal anemometer's detector was 8 μ. The results of these measurements, averaged along four points of the diameter, are shown in Figure 9.

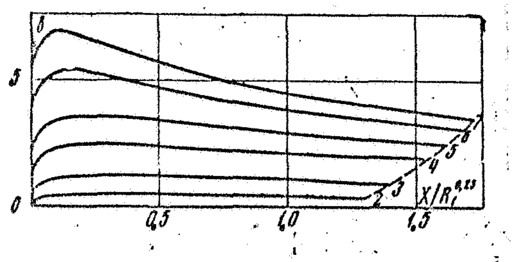

Fig. 7: The Change in the Permeability Factor b Along the Length of the Tube for Various Values of $j_1 R_1^{0.25}$

As we can see from these graphs, the mean filtration rate and, consequently, the permeability of the tube along its length can be assumed to be quite uniform.

The surface of the tube was practically smooth, since the relative roughness, equal to the ratio of the diameter of the particles, of which the tube is composed, to the radius of the tube was less than $3.6 \cdot 10^{-3}$.

The tube in the casing was reinforced by an intermediate element, foil. A fitting was welded on the top of the frame to measure the pressure on the entrance of air blown into the porous tube. Inside the frame collectors for the blown air were welded in diametrically positioned planes. The experimental section was attached to the forechamber. Due to the great convergence of the latter (100:1), the velocity profile at the entrance to the experimental section was uniform.

We measured the static and total pressure on the axis of the tube along its length by a specially constructed adjustable tube, whose construction is shown in Figure 8.

The diameter of the tube was 3 mm and its length was 400 mm. The adjustability of the tube along the axis of the operative section was provided by a coordinate spacer. Experiments were carried out in a stationary system. During the experiment we /28 measured the total and static pressure, the flow rates of the main and blown gas and the pressure in the receiving unit. As a pressure sensor we used a U-shaped piezometer filled with alcohol. The gas flow rate was measured by a specially calibrated measuring diaphragm. Pressure in the receiving unit was measured by a standard class 0.35 manometer.

The flow density of the blown gas was measured by two methods: by its flow rate across a measured disk and by the pressure drop on a sample. This was done to control possible leakages of the refrigerant at the places where the frame and the porous tube were joined. In all these experiments the comparison of these two independent measurements showed coinciding results (the maximum deviation between them was within the accuracy limits of the measurements).

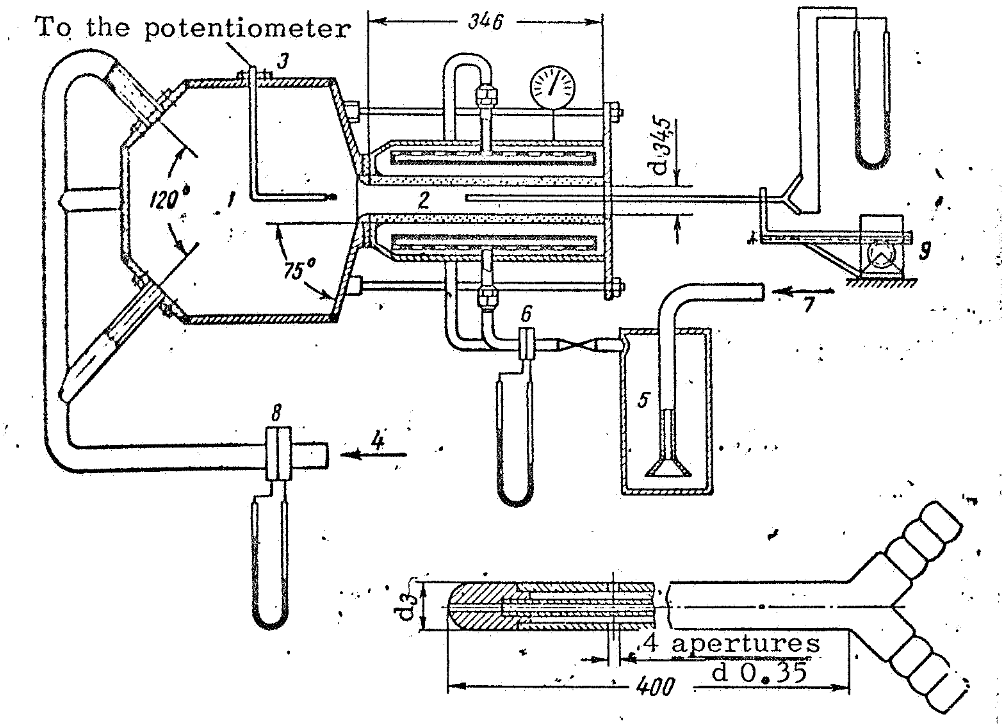

Fig. 8: Diagram of the Experimental Apparatus:
(1) The Forechamber; (2) The Experimental Section; (3) The Thermocouple; (4) The Main Gas Flow Rate Supply; (5) The Filter; (6) The Measuring Disk; (7) Refrigerant Supply; (8) The Measuring Disk of the Main Flow Rate; (9) The Coordinate Spacer.

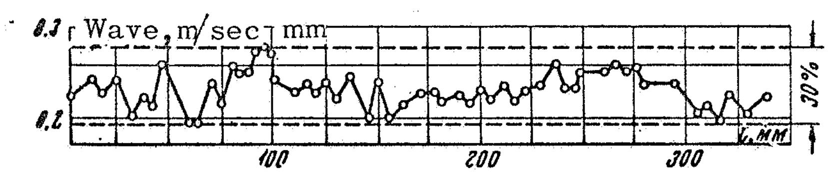

Fig. 9: Distribution of the Filtration Rate Averaged Along the Length of the Tube.

We computed the functions $\pi(\lambda)$ from the measured static and total pressure, and according to these functions we computed $q(\lambda)$. The value of the flow rate function and the Reynolds number at the entrance to the experimental section were computed by the flow rate of the main flow.

The variation range of the parameters in the process of the experiments consisted in terms of the Reynolds number, from $5.14 \cdot 10^4$ to $9.61 \cdot 10^4$ and in terms of the flow density $[(\rho w)_w/\rho_{01}w_{01}]R_1^{0.25}$ from 0 to 0.296. Figure 10 shows a comparison of the results of the /28 measurement of the velocity on the axis of the tube with various types of blowing and the calculation according to formulas (18) and (19). We can see that there is a satisfactory correlation between the assumed method of calculation and the experiment.

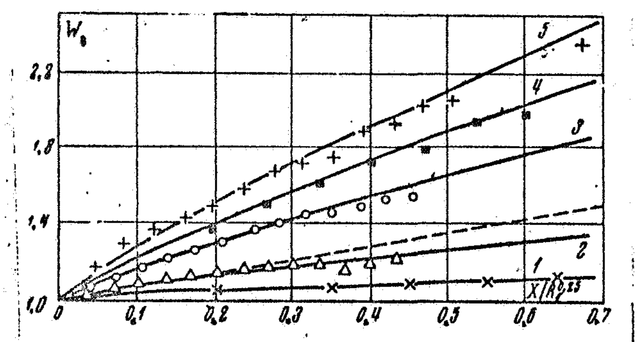

Fig. 10: The Change in the Relative Velocity Along the Length of the Initial Section: (1) $j_1 R_1^{0.25} = 0$; (2) 0.0553; (3) 0.174; (4) 0.029; (5) 0.296; the Solid lines Show the Calculation According to Equations (18)-(20); the Broken Lines Show the Calculation According to (21) for $j_1 R_1^{0.25} = 0.174$; the Dots Show the Experiment.

In the same graph the broken line shows the calculation of the change in velocity according to the continuity equation for a uniform flow when

$$W_{av} = 1 + 4 j_1 R_1^{0.25} X / R_1^{0.25}, \quad W_{av} = w_{av} / w_{01}. \tag{21}$$

This calculation was made for $j_1 R_1^{0.25} = 0.174$.

Figure 11 shows the distribution of the static pressure along the length of the tube for the same values of the parameter $j_1 R_1^{0.25}$. The calculation according to the proposed method was made by the formula

$$(P_{01} - P_0) / \rho_{01} w_{01} = {}^1/_2 (W_0^2 - 1), \tag{22}$$

where the values of the parameter W_0 were taken from the curve in Figure 10. This figure shows the results of the calculation of the static pressure distribution by a uniform procedure without taking friction into account. In this case the formula has the form

$$(P_{01} - P_0) / \rho_{01} w_{01} = W_{av}^2 - 1. \tag{23}$$

As we can see from the figure, the calculation by uniform procedure shows a noticeable divergence from the experiment.

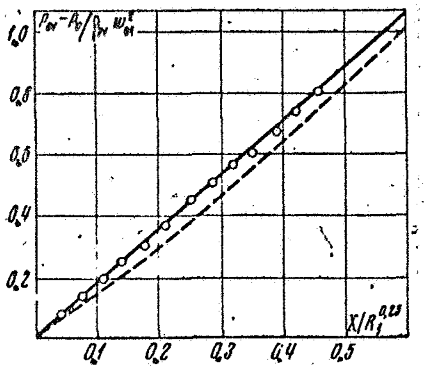

Fig. 11: The Static Pressure Distribution Along the Length of the Tube: the Solid Line Shows the Calculation According to Equation (22) for $j_1 R_1{}^{0.25} = 0.174$; the Broken Line Shows the Calculation According to (23); the Dots Show the Experiment.

Measurement of the velocity profile was made using a Prandtl tube, placed at a distance of 9.5 units from the entrance to the experimental section. The entrance aperture was made in the form of an ellipse with semiaxes of 0.175 and 0.30 mm. Adjustment of the tube was made by a coordinate spacer, and its position was determined by an MMN-1 cathetometer. Contact between the tube and the wall of the porous tube was registered by the completion of a special electric circuit. As a pressure sensor we used an MMN-1 micromanometer.

Using the known law of the change in velocity across the boundary layer, we integrated graphically the relationships for the thickness of the impulse loss and the displacement thickness.

Based on what we have discussed, we can propose the following sequence for calculating a turbulent boundary layer in the initial section of the tube.

(a) b = const, ψ_h = const;

(1) With the given values of b and ψ_h we should determine the parameters Ψ, H, δ^{**}/r_0 by formulas (4), (9) and (10).

(2) We should determine the length of the stabilization section X_H from equations (14) and (17).

(3) We should calculate the function $W_0 = f(X)$ from equation (14). /2

(4) We should compute the value of R^{**} from equation (13) and then compute the value of the coefficient of friction from equations (11) and (4).

(5) We should compute the required flow rate of blown gas from equation (3).

(b) $j_1 R_1^m$ = const.

(1) We should determine R^{**} and b from (18) and (20) with the assigned values of the parameter $j_1 R_1^m$, assigning a value to W_0.

(2) We should find the distribution of W_0 along the length of the initial section.

(3) We should find the length of the initial section from Figure 6.

(4) We should determine the coefficient of friction according to the known value of R^{**} from equations (11) and (4).

There would be no great difficulties in extending this method of calculation to include the case of a nonisothermic gas flow in the initial section of a porous tube. In this case we must take into account the influence of nonisothermicity on the friction law (4) and the shape factor H (10).

Notations

B is a constant; b is the permeability factor; c_f is the local coefficient of friction; D is the diameter of the tube; H is the shape factor; h is the enthalpy; j is the flow density; R is the Reynolds number; w is the velocity; W is the relative velocity; δ^* is the displacement thickness; δ^{**} is the thickness of the impulse loss; μ is the coefficient of dynamic viscosity; ρ is the density; x is the length of the tube; τ is the tangential stress; Ψ is the relative coefficient of fraction; ψ is the enthalpy factor; ξ is the relative coordinate.

Indices: 0 shows the parameters on the outer boundary of the boundary layer; 1 refers to the parameters at the entrance to the tube; w refers to the parameters on the wall; cr means critical; n refers to parameters on the boundary of the initial section; x refers to the parameters of the blown gas; h means thermal; av means average.

References

1. Olsen, R. and E. Eckhardt: Prakladnaya mekhanika, Vol. 88, No. 1, 1966.

2. Yuan, S.W., A. Barazotti: Heat Transfer and Fluid Mechanics Institute, No. 11, 1958, p. 25.

3. The Collection: Teplomassoobmen i treniye v turbulentnom pogranichnom sloye (Heat-Mass Exchange and Friction in a Turbulent Boundary Layer). S.S. Kutateladze, ed.), Sibirsk. otdeleniye Akad. Nauk SSSR, 1964.

4. Kutateladze, S.S. and A.I. Leont'yev: Turbulentnyy pogranichnyy sloy szhimayemogo gaza (Turbulent Boundary Layer of Compressible Gas). Sibirsk. Otdeleniye Akad. Nauk SSSR, 1962.

5. Mugalev, V.P.: Izv. Vysh. uchebn. zaved. Aviatsionnaya tekhnika, No. 3, 1959.

6. Mickley, H.S.: Rept NACA, 6228, 1955.

Translated for the National Aeronautics and Space Administration by:
Aztec School of Languages, Inc.
Research Translation Division (479)
Maynard, Massachusetts
NASW-1692